Precision Crystal Calorimetry in Future High Energy Colliders [1]

Ren-Yuan Zhu
California Institute of Technology, Pasadena, CA 91125

Abstract

Precision crystal calorimetry in future high energy physics experiments faces a new challenge to maintain its precision in a hostile radiation environment. This paper reviews the radition hardness requirements to the crystal scintillators and approaches to develop high quality scintillating crystals. Two on-going efforts are discussed in detail: the CsI(Tl) crystal development for the *BaBar* experiment at SLAC and the progress of the $PbWO_4$ crystal quality for the CMS experiment at LHC.

I. Introduction

Total absorption shower counters made of inorganic scintillating crystals have been known for decades for their superb energy resolution and detection efficiency. In high energy and nuclear physics, large arrays of scintillating crystals have been assembled for precision measurements of photons and electrons. The discovery potential of crystal calorimetry was early demonstrated by the Crystal Ball detector [1] through its study of radiative transitions and decays of the Charmonium family [2]. Over the last decade, following the Crystal Ball and CUSB [3] experiments, larger crystal calorimeters have been constructed, and their use has been a key factor in the successful physics programs of the L3 at LEP [4], of the CLEO II at CESR [5], of the Crystal Barrel at LEAR [6], and of KTeV at Tevatron [7].

Recently, several crystal calorimeters have been designed and are under development for the next generation of high energy colliders. These include CsI(Tl) calorimeters for two B Factory experiments: the *BaBar* experiment at SLAC [8] and the BELLE experiment at KEK [9], and a lead tungstate ($PbWO_4$) calorimeter for the Compact Muon Solenoid (CMS) experiment at the Large Hadronic Collider (LHC) [10]. Table 1 summarizes design parameters for these crystal calorimeters. One notes that each of these three calorimeters requires several cubic meters of high quality crystals.

The unique physics capability of crystal calorimetry is the result of its superb energy resolution, hermetic coverage and fine granularity [11]. In future high energy colliders, however, crystal calorimetry faces a new challenge: the radiation damage caused by the increased center of mass energy and luminosity. While the dose rate is expected to be a few rad/day for CsI(Tl) crystals at two B Factories, it would reach 1,000 rad/day for $PbWO_4$ crystals at LHC. In order to maintain high resolution *in situ*, crystals must be radiation hard enough and inter-calibrations must be able to follow crystal's change.

Table 1
Parameters of Recently Designed Crystal Calorimeters

Experiment	*BaBar*	BELLE	CMS
Laboratory	SLAC	KEK	CERN
Crystal Type	CsI(Tl)	CsI(Tl)	$PbWO_4$
B-Field (T)	1.5	1.0	4.0
Inner Radius (m)	1.0	1.25	1.44
Number of Crystals	6,580	8,800	110,000
Crystal Depth (X_0)	16 to 17.5	16.2	25
Crystal Volume (m^3)	5.9	9.5	13
Photosensor	Si PD	Si PD	APD[a]
Gain of Photosensor	1	1	50
$Area_{Photosensor}$ (cm^2)	4	4	0.2
Light Out (p.e./MeV)	5,000	5,000	2
Noise/Channel (MeV)	0.15	0.2	30
Dynamic Range	10^4	10^4	10^5

a Avalanche photodiode.

Section II gives a brief summary of scintillation crystals commonly used to construct crystal calorimetry and the radiation damage phenomena. Particular emphasis is given to the crystal radiation hardness requirements and approaches to develop high quality crystals. The development of radiation-hard CsI(Tl) crystals for the *BaBar* experiment is described in Section III. Section IV discusses the $PbWO_4$ crystal quality improvement for the CMS experiment. Finally, a summary and conclusions are given in Section V.

II. Crystals and Radiation Damage

A. Commonly Used Crystal Scintillators

Table 2 lists the basic properties of some heavy crystal scintillators: NaI(Tl), CsI(Tl), undoped CsI, BaF_2, CeF_3 (cerium fluoride), BGO and $PbWO_4$. All these crystals, except CeF_3 and $PbWO_4$, have been used in high energy physics experiments. Again, except CeF_3, all these crystals are available in large quantity. The expected price per cm^3 listed in the table corresponds to typical quotations of an order of more than 10^6 cm^3.

[1]Work supported in part by U.S. Department of Energy Grant No. DE-FG03-92-ER40701.

Table 2
Properties of Some Heavy Crystal Scintillators

	NaI(Tl)	CsI(Tl)	CsI	BaF_2	CeF_3	BGO	$PbWO_4$
Density (g/cm^3)	3.67	4.51	4.51	4.89	6.16	7.13	8.3
Melting Point (°C)	651	621	621	1280	1460	1050	1123
Radiation Length (cm)	2.59	1.85	1.85	2.06	1.68	1.12	0.9
Moliere Radius (cm)	4.8	3.5	3.5	3.4	2.6	2.3	2.0
Interaction Length (cm)	41.4	37.0	37.0	29.9	26.2	21.8	18
Refractive Index[a]	1.85	1.79	1.95	1.50	1.62	2.15	2.2
Hygroscopicity	Yes	slight	slight	No	No	No	No
Luminscence[b] (nm)	410	560	420	300	340	480	510
(at Peak)			310	220	300		510
Decay Time[b] (ns)	230	1300	35	630	30	300	50
			6	0.9	9		10
Relative LY[b,c]	100	45	5.6	21	6.6	9	0.3
			2.3	2.7	2.0		0.4
d(LY)/dT[b,d] (%/°C)	~0	0.3	−0.6	−2	0.14	−1.6	−1.9
				~0			
Price ($/cm^3$)	1 to 2	2	2.5	2.5	-	7	2[e]

a At the wavelength of the emission maximum.
b Top line: slow component, bottom line: fast component.
c Measured with a PMT with a bialkali cathode.
d At Room temperature.
e Quoted by russian industry to the CMS.

B. Requirements to Crystal's Radiation Hardness

All known large size crystal scintillators suffer from radiation damage. A common damage phenomenon is the appearance of radiation-induced absorption bands caused by color center formation. The absorption bands reduce crystal's light attenuation length [12], and hence the light output after irradiation. Additional damage effects may include a reduced intrinsic scintillation light yield (damage to the scintillation mechanism) and an increased phosphorescence (afterglow).

For crystals applicable to construct a precision calorimeter in severe radiation environment, two necessary conditions must be satisfied: (1) crystal's scintillation mechanism must not be damaged and (2) crystal's light attenuation length must be long enough so that the light response uniformity does not change *in situ*. Because of the nonuniform dose in crystals, caused by particle energy deposition at future colliders, a damage to the scintillation mechanism would cause distortion to the light response uniformity and thus unrecoverable degradation of the energy resolution [13]. On the other hand, if the light response uniformity is damaged by severe radiation-induced absorption, the degradation of energy resolution would also destroy the calorimeter's resolution.

Data presented in this paper shows that the crystal's light response uniformity does not change after irradiation when its initial light attenuation length is long enough. This is true not only for the case when radiation dose was applied uniformly to the entire volume of the crystal (Section IV), but also for the case when only a part of the crystal volume suffers from radiation dose (Section III). This phenomenon can be understood by the light propagation in crystals, since the intensity of all light rays attenuates equally after passing the same radiation-induced absorption zone in the crystal. This has also been explained by a ray-tracing simulation [14].

With these two necessary conditions satisfied, the next important issue is the stability of crystal's light output. It is known that impurities and point defects in crystals create color centers which cause radiation-induced absorption. It is also known that radiation-induced color centers with shallow trap depth may annihilate at room temperature, causing the recovery. The kinetics of color center creation and annihilation in crystals is well described by first order differential equation, as extensively studied for the case of BaF_2 optical bleaching [15]. The kinetic nature of these color centers, however, would lead to unstable light output *in situ*. For precision crystal calorimetry, it is important to understand the differential change of crystal's light output *in situ*, i.e., its degradation under irradiation and its spontaneous recovery at room temperature. It is also important to understand the inter-calibration means available in the experiment and how frequently they may be applied to follow the differential change of crystal's light output. The radiation hardness specification, therefore, should be defined by taking all above information into account.

Last, the effect of the radiation-induced phosphorescence should also be checked to make sure that the additional noise would not degrade the readout.

In a brief summary, the following three key issues are to be systematically investigated for crystals to be used to construct precision calorimetry.

1. Possible damage in crystal's scintillation mechanism.
2. Degradation of light attenuation length after irradiation and its consequence to the light response uniformity.
3. Degradation of crystal's light output under expected dose and its recovery at room temperature.

C. Approaches to Improve Crystal's Quality

Crystals produced by manufactures are usually not up to the quality required by precision crystal calorimetry. A research and development program is usually needed to develop high quality crystals. A systematic approach has been adapted in the past to improve quality of BGO crystals for L3 [16] and of BaF_2 crystals for L* and GEM [13], which lead to significant progress of crystal quality.

This approach is to study the correlations between radiation hardness and the impurities and point defects in the crystal. It includes three parts:

1. investigate full size samples to understand any changes in the optical properties of the crystal under irradiation, including emission, transmittance, light attenuation length, light output, decay time and light response uniformity;
2. study the correlation between radiation damage and impurities and/or point defects in the crystal using various types of material analysis; and
3. define procedures for removing harmful impurities from the raw materials, and search for ways to reduce the density of defects in the crystal during growth and processing.

Recently, this approach has also been adapted to develop CsI(Tl) crystals for *BaBar* [17] and $PbWO_4$ crystals for CMS [18].

III. Cesium Iodide Development for *BaBar* Experiment at SLAC

For CsI(Tl) crystals in the *BaBar* experiment, the dominant radiation dose comes from 500 keV photons, which penetrate only the first few cm in the crystal. The expected dose rate for CsI(Tl) crystals at PEP-II Asymmetric Collider is 45 and 90 rad/year at $\theta = 90°$ (barrel) and 17° (endcap) respectively, during luminosity runs. Including also injections and machine studies, the dose rate is estimated to be 500 and 1,500 rad/year at r = 100 (barrel) and 45 cm (endcap), respectively [8].

The radiation damage of CsI(Tl) crystals have been extensively studied [19, 20, 17]. The corresponding radiation hardness specification for CsI(Tl) crystals was defined for the *BaBar* experiment. It requires that crystal's light output after irradiation should be better than 97, 90 and 80% for accumulated dose of 10, 100 and 1,000 rad, which corresponds to a daily degradation of crystal light output of less than 0.15 and 0.3% in the barrel and endcap, respectively.

This specification was defined based upon the following facts: (1) the scintillation mechanism of CsI(Tl) is not damaged; (2) the change of light response uniformity is negligible up to 10 krad, if crystal's initial light attenuation length is long enough; (3) the spontaneous damage recovery is extremely slow at room temperature; and (4) the inter-calibration for CsI(Tl) crystals will be provided by Bhabha events every few hours.

A. CsI(Tl) Samples

A total of 20 CsI(Tl) samples were investigated. 16 full size samples were originated from four crystal producers: Beijing Glass Research Institute (BGRI) [21] in Beijing, Crismatec [22] in France, ITC (Khar'kov) [23] in the Ukrain, and Shanghai Institute of Ceramics (SIC) [24] in Shanghai. In addition, four test samples were prepared by SIC with different levels of scavenger 095 in the melt. All full sized samples have a tapered shape (4.5×4.5 cm^2 at the small end, tapering to 6.0×6.0 cm^2 at the large end,

Table 3
CsI(Tl) Samples Investigated in this Report

ID	Dimension (cm)	Material	Method
Khar'kov-1	$4.5^2 \times 33.5 \times 6^2$	Russian	Czoc.
Khar'kov-2	$4.5^2 \times 33.5 \times 6^2$	Russian	Czoc.
BGRI-1	$4.5^2 \times 29 \times 5^2$	Chemetall	Brid.
BGRI-2	29.5 cm long	Chemetall	Brid.
SIC-1	$5^2 \times 28 \times 5.5^2$	Chemetall	Brid.
SIC-2	$5^2 \times 28 \times 6^2$	Chemetall	Brid.
SIC-4	$4.2^2 \times 30 \times 5.4^2$	APL	Brid.
SIC-5[a]	$4.6^2 \times 29 \times 5.8^2$	Chemetall	Brid.
SIC-6[a]	$5.0^2 \times 26 \times 6.0^2$	APL	Brid.
SIC-7[a]	$4.8^2 \times 27 \times 5.8^2$	APL	Brid.
SIC-8[a,b]	$4.8^2 \times 26 \times 6.0^2$	APL	Brid.
Crismatec-1	$4.7^2 \times 30 \times 6^2$	APL	Kyrop.
Crismatec-2	$4.7^2 \times 30 \times 6^2$	APL	Kyrop.
Crismatec-3	$4.7^2 \times 30 \times 6^2$	APL	Kyrop.
Hilger-16	$5.5^2 \times 25 \times 6.6^2$	APL	Kyrop.
Hilger-19	$5.5^2 \times 25 \times 6.6^2$	APL	Kyrop.
ID	Dimension (mm)	095 (ppm)	Method
SIC-T1	$14^2 \times 29 \times 14^2$	0	Brid.
SIC-T2	$14^2 \times 29 \times 14^2$	100	Brid.
SIC-T3	$14^2 \times 29 \times 14^2$	500	Brid.
SIC-T4	$14^2 \times 29 \times 14^2$	1,000	Brid.

a. A proprietary Scanvenger (095) used in the melt.
b. Reverse cut to improve light response uniformity.

and >28 cm long). Table 3 lists the dimensions, the raw material used and the growing method for these samples, where Czoc., Brid. and Kyrop. represent Czochralski, Bridgman and Kyropolous method, respectively.

Only damage by electromagnetic energy deposition using ^{60}Co γ-rays was measured. For full size samples, the irradiation was uniformly applied to the front (small) face of the crystal only, i.e., all side faces were shielded to simulate the situation *in situ* at PEP-II.

B. CsI(Tl) Radiation Damage

The scintillation mechanism of CsI(Tl) crystals is not damaged. The degradation of light output is due only to the radiation-induced absorption, i.e., color center formation. This conclusion is drawn based on the following facts: (1) no change in the shape of emission spectrum; (2) no change in the scintillation decay time; and (3) negligible damage in the light response uniformity, if crystal's initial light attenuation length is long enough.

Figure 1 shows the photo-luminescence spectra before and after 1 krad irradiation for three full size samples. Within the measurement errors, the shape of these emission spectra are identical.

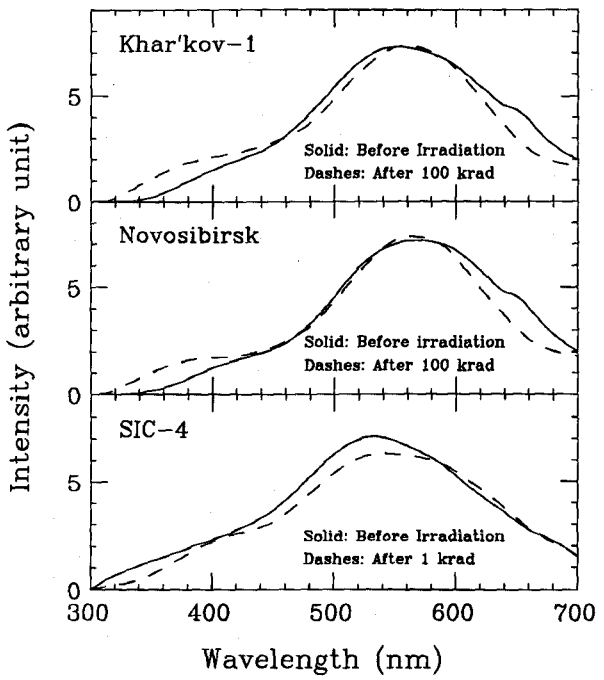

Fig. 1 CsI(Tl) photoluminescence before and after irradiation.

Figure 2 shows the light response uniformity as a function of accumulated dose for a full size sample. The pulse heights measured in nine points evenly distributed along the longitudinal axis of the crystal is fit to a normalized function:

$$LY/LY_{mid} = 1 + \delta(x - x_{mid})/x_{mid}, \qquad (1)$$

where x is the distance from the small end, LY_{mid} is the fit value of the light yield at the middle of the crystal, x_{mid}, and δ is a measure of the light response uniformity. This

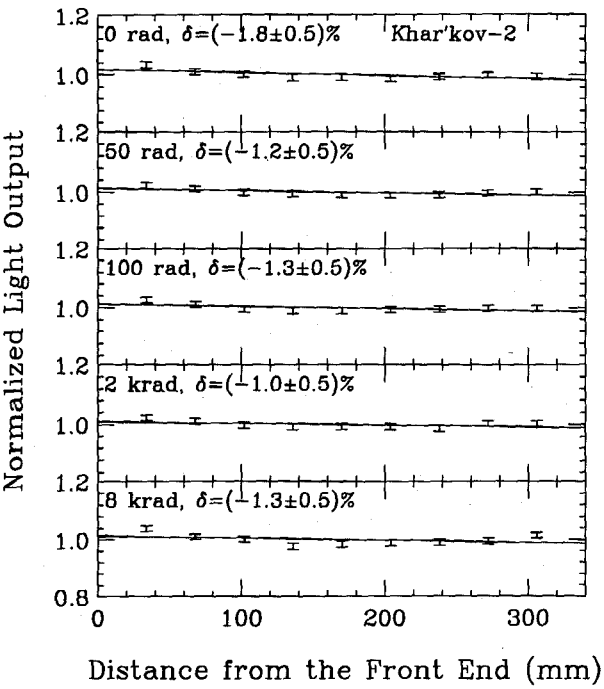

Fig. 2 CsI(Tl) light response uniformity as a function of accumulated dose.

figure shows clearly that the slope (δ) and the shape of the uniformity does not change up to 10 krad, although only the front few cm of the crystal absorbed the radiation dose.

The CsI(Tl) damage recovery at room temperature is very slow. Figure 3 shows the recovery speed of less than 0.5% per day for three full size samples after irradiation.

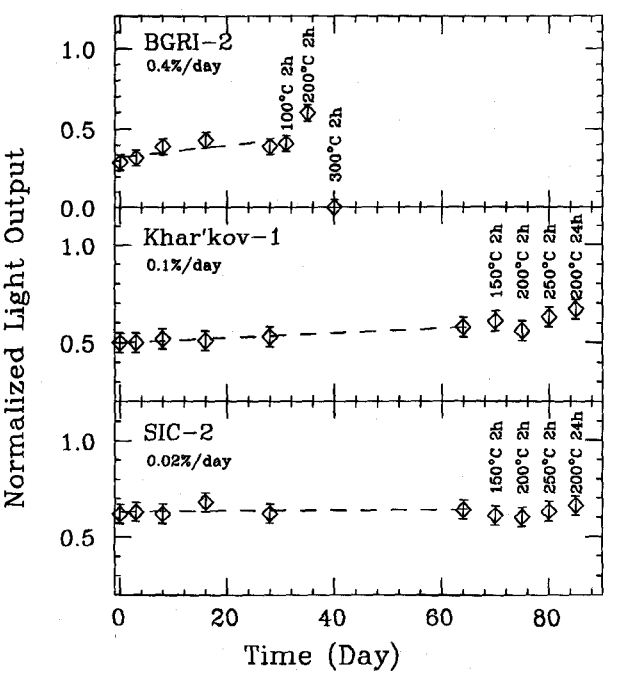

Fig. 3 CsI(Tl) light output recovery as a function of time after irradiation.

This figure also indicates that the radiation-induced color centers in CsI(Tl) are deep, since thermal annealing below 300°C did not accelerate recovery. In addition, thermal annealing beyond 300°C made sample BGRI-2 turned milky and produced no more scintillation light. This can be explained by an assumption that at high temperature the thallium luminescence centers drift out of the CsI(Tl) lattice. Because of this slow recovery, the inter-calibration may be provided by physics, e.g., Bhabha events, *in situ* in a few hours, during which there will be no serious light output change.

C. CsI(Tl) Crystal Development

Early CsI(Tl) samples produced at SIC did not satisfy *BaBar* specification. Glow Discharge Mass Spectroscopy (GDMS) was used to identify trace element impurities in the crystal. Impurities were detected in a portion of each sample, taken 3 to 5 mm below the surface of the crystal. A survey of 76 elements, including all of the lanthanides, indicated that there was no obvious correlation between the detected trace impurities, e.g., the sum of transition metals and the sum of rare earth elements, and the crystal's susceptibility to radiation damage. This indicates that oxygen, which was unable to be measured by the GDMS analysis, might play an important role.

Oxygen contamination is known to cause radiation damage for other alkali halide scintillators. In BaF_2, for example, hydroxyl (OH^-) may be introduced into crystal through a hydrolysis process, and latter decomposed to interstitial and substitutional color centers by radiation

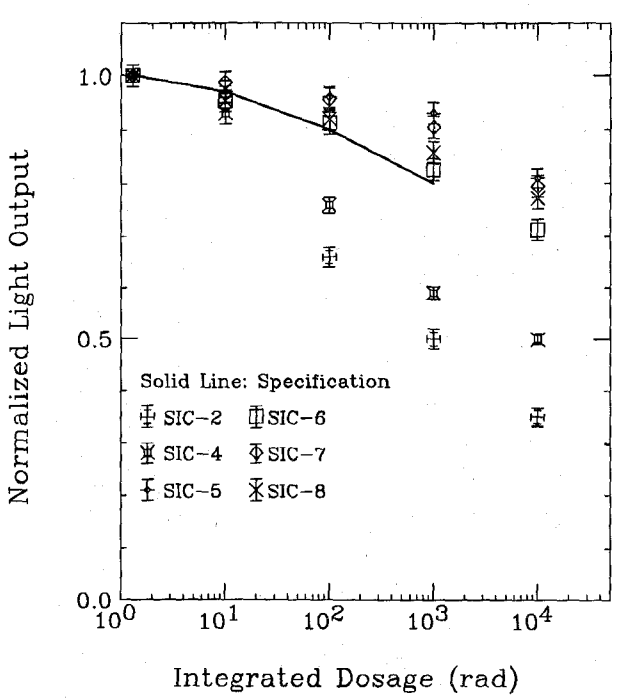

Fig. 4 Progress of CsI(Tl) radiation hardness is shown as the light output as a function of accumulated dose.

through a radiolysis process,

$$OH^- \rightarrow H_i^0 + O_s^- \quad or \quad H_s^- + O_i^0 \qquad (2)$$

where subscript i and s refer to interstitial and substitutional centers respectively [13]. Both the O_s^- center and the U center (H_s^-) were identified.

Following BaF_2 experience, effort was made to remove oxygen contamination in CsI(Tl). Two approaches were tried at SIC: a better seal of the platinum crucible and a use of a scavenger, such as Pb for BaF_2. The second approach was tested in an experiment with four small test samples listed in Table 3. Significant improvement of radiation hardness was observed for samples with scavenger 095 in the melt [17]. Consequently, this technique is used in growing full size samples. Figure 4 shows the CsI(Tl) light output as a function of accumulated dose compared to the *BaBar* radiation hardness specification (solid line). While samples SIC-5, 6, 7 and 8 (with scavenger 095) satisfy the *BaBar* specification, early samples SIC-2 and 4 did not. It is understood that the function of the scavenger is to form oxide with density less than CsI, so that the oxide will migrate to the top of the ingot during the growing process, similar to the zone-refining process. By doing so, both oxygen and scavenger are removed from the crystal.

IV. Lead Tungstate Quality Improvement for CMS at LHC

For $PbWO_4$ crystals in the CMS experiment, the dominant radiation dose originates from the high energy deposition in the crystal. The expected dose rate at LHC is 3 to 5 rad/hr and 2×10^8 neutrons/hr/cm^2 at low luminosity of 10^{33} s^{-1} cm^{-2}, and 12 to 50 rad/hr and 20×10^8 neutrons/hr/cm^2 at high luminosity of 10^{34} s^{-1} cm^{-2} [10].

The $PbWO_4$ crystals have been extensively studied recently [25, 26, 27, 28, 18]. The study on $PbWO_4$ radiation damage is currently under way by the CMS collaboration, and the radiation hardness specification is yet to be defined. It is expected that the final specification would require (1) a tolerable saturated light output loss, e.g., a few percent, at the dose rate expected at LHC and (2) a long enough degraded light attenuation length to maintain crystal's light response uniformity.

The concept of this specification is based upon the following facts: (1) the scintillation mechanism of $PbWO_4$ is not damaged; (2) the change of light response uniformity is negligible up to a few Mrad for crystals with good quality, or long initial light attenuation length; (3) there is a shallow color center causing fast spontaneous recovery at room temperature; and (4) the inter-calibration for $PbWO_4$ crystals may be provided by continuous light monitoring.

The absolute calibration of $PbWO_4$ calorimeter *in situ* will be provided by physics (W and Z events) every few weeks. The continuous inter-calibration provided by the

light monitoring will track the residual damage and its recovery by injecting light pulses into crystals in the 3.17 μs beam gap every 88.924 μs during LHC operation [29].

A. $PbWO_4$ Samples

A total of 18 $PbWO_4$ samples were investigated. Nine large size samples were originated from two crystal producers: Bogoroditsk Techno-Chemical Plant (BTCP) and SIC. In addition, several test samples were prepared by SIC with an additional annealing process in different atmospheres, e.g., air, argon gas, oxygen gas and vacuum, while most crystals from BTCP were doped with niobium. The final full sized crystal for CMS $PbWO_4$ calorimeter should have a tapered shape (2.0×2.0 cm^2 at the small end, tapering to 2.4×2.4 cm^2 at the large end, and 23 cm long). Table 4 lists the dimensions, growing method and special features for these samples.

Only damage by electromagnetic energy deposition using ^{60}Co γ-rays was measured. The irradiation was uniformly applied to the entire volume of the crystal to simulate the situation *in situ* at LHC.

Table 4
$PbWO_4$ Samples Investigated in this Report

ID	Dimension (cm)	Method	Remark
BTCP-478	$0.8 \times 1.0 \times 1.0$	Czoc.	–
BTCP-728	$1.8^2 \times 21.3 \times 2.1^2$	Czoc.	–
BTCP-767	$1.8^2 \times 21.3 \times 2.1^2$	Czoc.	Nb-dop.
BTCP-768	$1.8^2 \times 21.3 \times 2.1^2$	Czoc.	Nb-dop.
BTCP-1015	$1.8^2 \times 21.3 \times 2.1^2$	Czoc.	Nb-dop.
BTCP-1022	$1.8^2 \times 21.3 \times 2.1^2$	Czoc.	Nb-dop.
BTCP-1018	$1.8^2 \times 21.3 \times 2.1^2$	Czoc.	Nb-dop.
BTCP-1031	$1.8^2 \times 21.3 \times 2.1^2$	Czoc.	Nb-dop.
SIC-4	$\phi 3 \times 4.5$	Czoc.	–
SIC-10	$2.5 \times 2.5 \times 2.5$	Brid.	–
SIC-17	$2.5 \times 2.5 \times 2.5$	Czoc.	–
SIC-34	$2.5 \times 2.5 \times 4.5$	Brid.	Vac. A.
SIC-41	$2.0 \times 2.1 \times 2.5$	Brid.	O_2 A.
SIC-64	$1.7 \times 8.5 \times 2.0$	Brid.	Ar A.
SIC-65	$2.0 \times 5.4 \times 2.0$	Brid.	Air A.
SIC-66	$1.9 \times 17 \times 1.9$	Brid.	O_2 A.
SIC-67	$1.8 \times 9.8 \times 2.2$	Brid.	Vac. A.
SIC-85	$2.0 \times 20 \times 2.3$	Brid.	O_2 A.

B. $PbWO_4$ Radiation Damage

The scintillation mechanism of $PbWO_4$ crystals is not damaged. The degradation of light output is due only to the radiation-induced absorption, i.e., color center formation. This conclusion is drawn based on the following facts: (1) no change in the shape of emission spectrum; (2) no change in the scintillation decay kinetics; and (3) negligible damage in the light response uniformity, if crystal's initial light attenuation length is long enough.

Figure 5 shows the photo-luminescence spectra before and after 1 krad irradiation for three large samples.

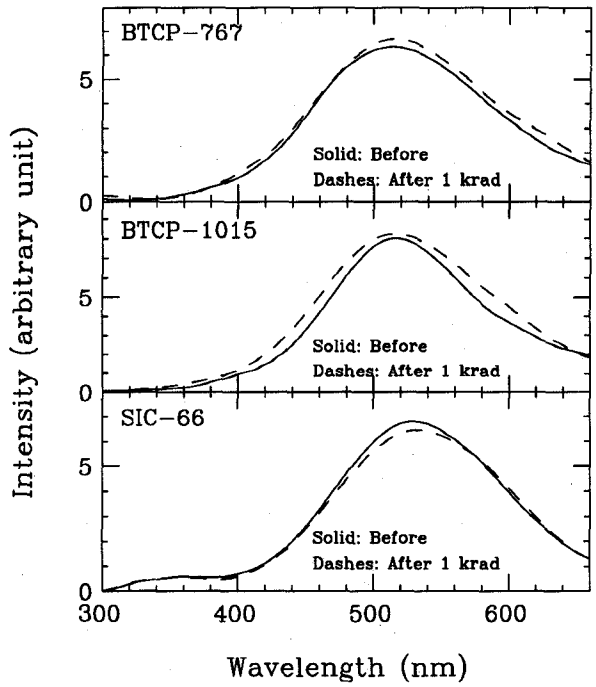

Fig. 5 $PbWO_4$ photoluminescence before and after irradiation.

Within the measurement errors, the shape of these emission spectra are identical.

Figure 6 shows the light response uniformity as a function of accumulated dose for sample SIC-85, where δ is a measure of the light response uniformity, as defined in Equation 1. This figure shows clearly that the slope (δ) and the shape of the uniformity does not change up to 2.2 Mrad, indicating an adequate light attenuation length

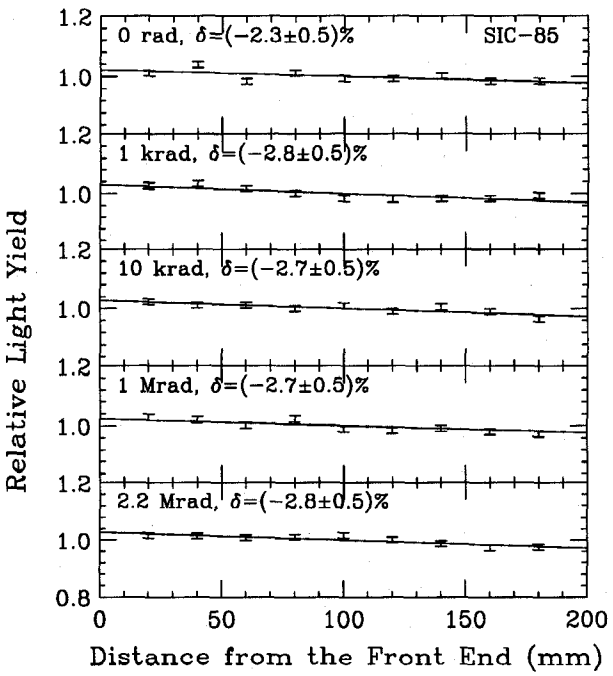

Fig. 6 $PbWO_4$ light response uniformity as a function of accumulated dose.

both before and after irradiation.

At least two types of color centers were found, and they follow color center kinetics. Figure 7 shows the entire history of the light output normalized to the value before irradiation for sample SIC-85. This is an extensive experiment carried out step by step with ten irradiations of accumulated doses of 0.01, 0.1, 1, 10, 20, 55, 100, 1,000, 1,600 and 2,200 krad. In the entire period of 50 days, the light output was continuously measured except during irradiation. Note, the first six irradiations were applied with a dose rate of 0.48 krad/hr and the last four of 36 krad/hr.

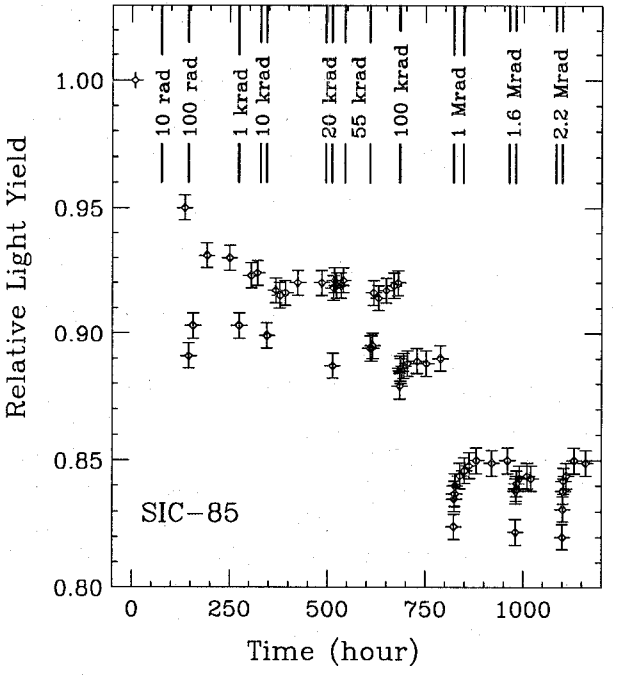

Fig. 7 $PbWO_4$ light output history as a function of time for ten irradiations.

Figure 8 shows fits to the recovery time constant. The light output as a function of time after irradiation was fit to a fast recovery component with a time constant of τ and an amplitude of A_f, and a slow recovery component with an amplitude of A_s.

$$LY = LY_0(1 - A_s - A_f e^{-t/\tau}) \tag{3}$$

This analysis revealed that there exists a shallow color center with a fast recovery time constant of about one hour and an additional deep center with much longer recovery time constant. In addition, the analysis also revealed that while the damage caused by the shallow center saturates at the level of about 3% of the original light output and is dose rate independent, the damage caused by the deep center changes from 7 to 8% for dose rate of 0.48 krad/hr to 15 to 16% for 36 krad/hr. For each fixed dose rate, the damage saturates when accumulated dose increases, as shown in Figure 7.

This damage phenomenon shown in Figure 7 can be

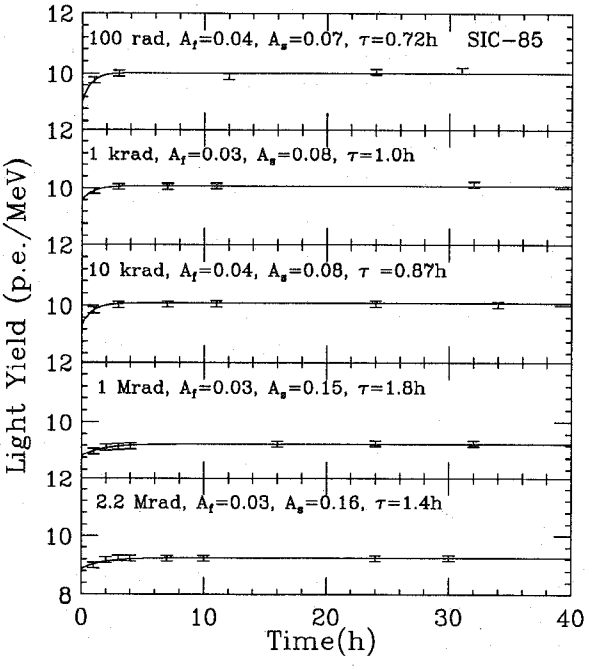

Fig. 8 $PbWO_4$ light output recovery as a function of time after irradiation.

understood by the balance of two processes: the color center creation (irradiation) and annihilation (room temperature annealing). Assuming the annilation speed of color center i is proportional to a constant a_i and its creation speed is proportional to a constant b_i and the dose rate (R), the differential change of color center density when both processes exist can be expressed as [15]:

$$dD = \sum_{i=1}^{n} \{-a_i D_i dt + (D_i^{all} - D_i)\, b_i R dt\} \tag{4}$$

where D_i is the density of the color center i in the crystal and the summation goes through all centers.

The solution of Equation 4 is

$$D = \sum_{i=1}^{n} \{\frac{b_i R D_i^{all}}{a_i + b_i R}\, [1 - e^{-(a_i + b_i R)t}] + D_i^0 e^{-(a_i + b_i R)t}\} \tag{5}$$

where D_i^{all} is the total density of the trap related to the center i and D_i^0 is its initial density. The color center density in equilibrium (D_{eq}) indeed depends on the dose rate (R).

$$D_{eq} = \sum_{i=1}^{n} \frac{b_i R D_i^{all}}{a_i + b_i R} \tag{6}$$

Equation 6 also explains why the damage level in equilibrium has no dose rate dependence for a shallow center (large b), while it does for a deep center (small b).

In summary, with the present $PbWO_4$ crystal quality, continuous inter-calibration is the only solution to track the change of crystal's light output. Further improvement of crystal quality is certainly needed, and the goal is to

reduce D^{all} to an acceptable level. Note, the most harmful color center to the stability of $PbWO_4$ calorimeter *in situ* at LHC is the shallow one with fast recovery.

Finally, optical bleaching is effective in eliminating color centers in $PbWO_4$, damage by UV light can also exist [18]. Therefore, the color center density in $PbWO_4$, or crystal's light attenuation length, may be fine tuned *in situ* by using monitoring system to deliver bleaching/damage light to the crystal.

C. $PbWO_4$ Quality Improvement

$PbWO_4$ samples produced have very different radiation hardness. Particle Induced X-ray Emission (PIXE) and quantitative wavelength dispersive Electron MicroProbe Analysis (EMPA) were used to identify possible deviations from stoichiometric $PbWO_4$ for samples from BTCP. Crystals were found essentially pure stoichiometric $PbWO_4$. However, there was an indication that the W/Pb ratio decreased by up to a few percent from the small end to the large end for some crystals.

Glow Discharge Mass Spectroscopy (GDMS) was also used to identify trace elements impurities. Similar to the CsI(Tl), the result of the GDMS analysis indicated that there was no obvious correlation between the detected trace impurities and the crystal's susceptibility to radiation damage. This indicates that defects in the crystal, such as oxygen vacancies, which were unable to be measured by the GDMS analysis, may play an important role.

Oxygen vacancies may also play an important role in BGO radiation damage. Our previous study identified three radiation-induced color centers in BGO peaked at 2.3, 3.0 and 3.8 eV, common for all samples doped with different impurities [30]. Following the BGO experience, effort was made to reduce the density of oxygen vacancies in $PbWO_4$. An approach was tried at SIC to compensate oxygen vacancies by an additional annealing process in an oxygen-rich atmosphere. This approach was tested in an experiment with four test samples (SIC-64, 65, 66 and 67) listed in Table 4. Significant improvement of radiation hardness was observed for samples annealed in oxygen [18]. Consequently, this technique was used in full size samples. Figure 9 shows $PbWO_4$ light output as a function of accumulated dose for two large samples: SIC-66 produced in January, 1996 and SIC-85 in August, 1996. A factor of two improvement in radiation resistance is observed by refining the annealing process. Effort is being made to further reduce the oxygen vacancies.

It is also interesting to note that the GDMS analysis does reveal a possitive correlation between the molybdenum contamination and the fraction of slow scintillation component. Figure 10 shows the Mo concentration in ppm versus the fraction of light measured in 100 ns gate for six BTCP samples. A similar observation was reported by M. Kobayashi [26]. This correlation is easy to be understood, since lead molybdate ($PbMoO_4$) is a known scintillator with slow ($\sim$10 μs) decay time. After removing Mo and other cation contamination from the raw material, $PbWO_4$ crystals produced at both BTCP and SIC in 1996 have a significantly reduced slow component.

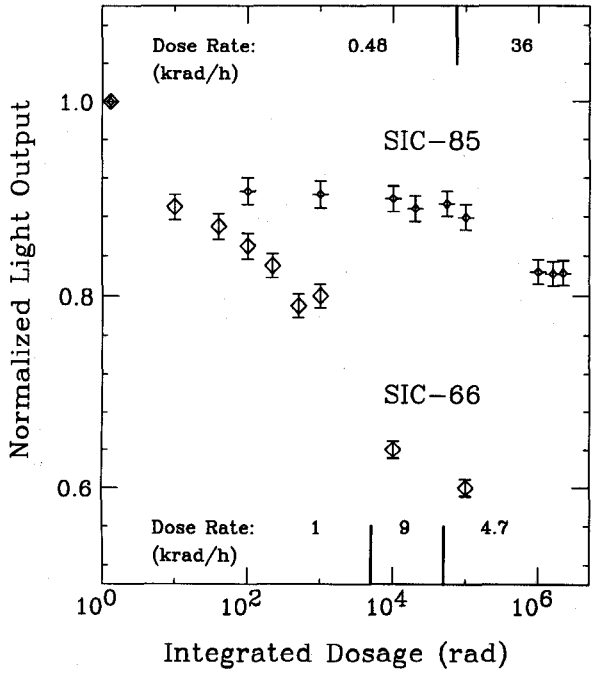

Fig. 9 Improvement of $PbWO_4$ radiation hardness is shown as the light output as a function of accumulated dose.

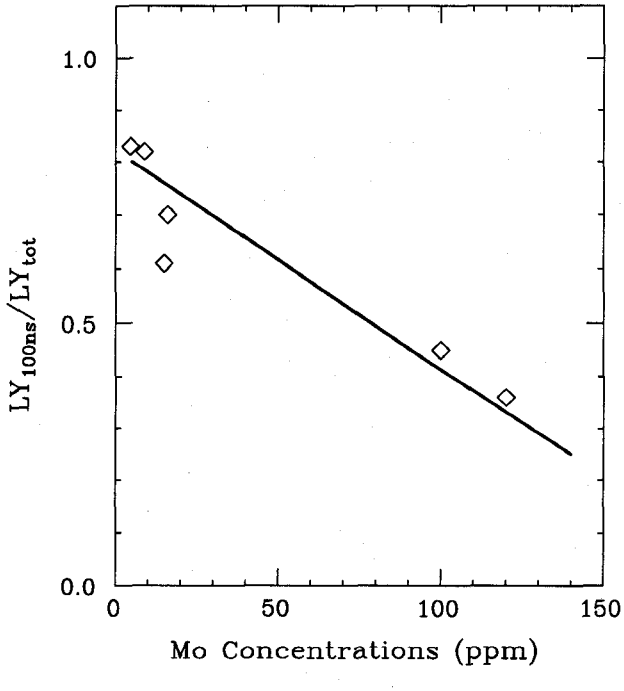

Fig. 10 The correlation between Mo contamination and the fraction of fast scintillation component.

V. Summary and Conclusions

Despite much experience and expertise accumulated in the last decade, crystal calorimetry in high energy physics is facing a new challenge. Crystals in future high energy colliders will operate in a severe radiation environment caused by increased center of mass energy and luminosity. Without stringent quality control, crystals would suffer from significant radiation damage, and thus leading to a much degraded performance.

Possible effects of radiation damage in a scintillating crystal include (1) radiation induced absorption; (2) damage in scintillation mechanism and (3) radiation induced phosphorescence. However, most scintillation crystals do not suffer from scintillation mechanism damage and its light response uniformity does not change if initial light attenuation length is long enough. This provides a foundation to use light monitoring as inter-calibration *in situ*, even if crystals suffer from radiation-induced light output loss.

Much effort has been devoted to the crystal quality control, especially to the investigation and improvement of crystal's radiation resistance. It is understood that stringent specifications for CsI(Tl) crystals to be used to construct calorimeters for two B Factories can be satisfied. On the other hand, full size $PbWO_4$ crystals suffer from non-negligible radiation damage after a radiation dose as low as 10 rad. Although the $PbWO_4$ crystal quality improvement reported in this paper is significant, further research and development, however, is still needed to control and improve the quality of mass produced $PbWO_4$ crystals.

We are also confident that the quality of mass production crystals may be improved through a systematic research and development program carried out by a close collaboration between physicists and crystal producers. The development of scaveger 095 for CsI(Tl) crystals and the oxygen annealing for $PbWO_4$ quality improvement are two examples.

VI. Acknowledgements

Mr. Q. Deng, D.A. Ma and H. Wu performed delicated measurements described in this report. Prof. Z.W. Yin provided CsI(Tl) and $PbWO_4$ samples produced at SIC. Dr. P. Lecoq provided $PbWO_4$ samples grown at BTCP. The $PbWO_4$ work described in this report is a part of collaborative research with C. Woody of Brookhaven National Laboratory. Many inspiring and interesting discussions with Drs. E. Auffray, B. Borgia, G. Eigen, D. Hitlin, M. Kobayashi, M. Korzhik, P. Lecoq, J.Y. Liao, A. McKemey, H. Newman, M. Nikl, J. Reidy, M. Schneegans, D.Z. Shen, J. Virdee, C. Woody, and Z.W. Yin are also acknowledged.

VII. References

[1] M. Oreglia *et al.*, *Phys. Rev. D* 25 2295 (1982).
[2] E. Bloom and C, Peck, *Ann. Rev. Nucl. Part. Sci.* 33 143-197 (1983).
[3] T. Böringer *et al.*, *Phys. Rev. Lett.* 44: 1111 (1980); G. Mageras *et al.*, *Phys. Rev. Lett.* 46: 1115 (1981).
[4] L3 Collaboration, *Nucl. Instr. and Meth.* A289 35 (1990).
[5] Y. Kubota *et al.*, *Nucl. Instr. and Meth.* A320 66 (1992).
[6] E. Aker *et al.*, *Nucl. Instr. and Meth.* A321 69 (1992).
[7] K. Arisaka *et al.*, *KTeV Design Report*, FN-580, January (1992).
[8] *BaBar* Collaboration, *Technical Design Report*, SLAC-R-95-457 (1995).
[9] BELLE Collaboration, *Technical Design Report*, KEK Report 95-1 (1995).
[10] *Compact Muon Solenoid Technical Proposal*, CERN/LHCC 94-38 (1994).
[11] R.Y. Zhu *et al.*, *Nucl. Phys.* B44 547 (1995).
[12] D.A. Ma and R.Y. Zhu, *Nucl. Instr. and Meth.* A333 (1993) 422.
[13] R.Y. Zhu, *Nucl. Instr. and Meth.* A340 442 (1994).
[14] R.Y. Zhu, talk presented in CMS ECAL meeting, August (1995), to be submitted to *Nucl. Instr. and Meth.*.
[15] D.A. Ma and R.Y. Zhu, *Nucl. Instr. and Meth.* A332 113 (1993) and D.A. Ma *et al.*, *Nucl. Instr. and Meth.* A356 309 (1995).
[16] Z.Y. Wei *et al.*, *Nucl. Instr. and Meth.* A297 163 (1990).
[17] R.Y. Zhu, CALT-68-2072, will be in *Proceedings of VI International Conference on Calorimetry in High Energy Physics*, Frascati, June (1996).
[18] R.Y. Zhu *et al.*, *Nucl. Instr. and Meth.* A376 319 (1996); C. Woody *et al.*, in *International Conference on Inorganic Scintillator and Their Applications*, Delft (1995) and in IEEE/NSS, San Fracisco (1995); and R. Zhu *et al.*, CALT-68-2071, to be published in *Proceedings of VI International Conference on Calorimetry in High Energy Physics*, Frascati (1996).
[19] D. Hitlin and G. Eigen, in *Heavy Scintillators*, Editions Frontieres, ed. F. Nataristefani *et al.*, p. 467 (1992).
[20] C.L. Woody *et al.*, *IEEE Trans. Nucl. Sci.* NS-39 524 (1992).
[21] Beijing Glass Research Institute is a reasearch institution in Beijing, 1 Dongdadi Chongwenmen Wai, Beijing 100062, China.
[22] The Crismatec is a subsidiary of Sant-Gobain Ceramics Industries in France.
[23] The ITC is the former Institute of Single Crystal Research in Khar'kov, Ukrain.
[24] Shanghai Institute of Ceramics is a reasearch institution belong to the Chinse Academy of Sciences, 1295 Ding Xi Road, Shanghai 200050, China.
[25] P. Lecoq *et al.*, *Nucl. Instr. and Meth.* A365 (1995) 291.
[26] M. Kobayashi *et al.*, *Nucl. Instr. and Meth.* A373 (1996) 333.
[27] M. Korzhik *et al.*, *Phys. Stat. Sol.* a154 (1996) 779 and A. Annenkov *et al.*, *Phys. Stat. Sol.* a156 (1996) 493.
[28] M. Nikl *et al.*, *Phys. Stat. Sol.* b195 (1996) 311. and *Phys. Stat. Sol.* b196 (1996) K7.
[29] The LHC Study Group, CERN/AC/95-05 46 (1995).
[30] R.Y. Zhu *et al.*, *Nucl. Instr. and Meth.* A302 69 (1991).